Synthesis, Langmuir and Langmuir-Blodgett films of a calix[7]arene ethyl ester.

J. Torrent-Burgués

Department of Chemical Engineering, Universitat Politècnica de Catalunya

C/ Colom 1, 08222 Terrassa (Barcelona), Spain, juan.torrent@upc.edu

F. Vocanson

Université de Lyon, F-42023, Saint-Etienne, France; CNRS, UMR 5516, Laboratoire Hubert Curien, F-42000, Saint-Etienne, France; Université de Saint-Etienne, Jean Monnet, F-42000, Saint-Etienne, France

J.J. Pérez-González

Department of Chemical Engineering, Universitat Politècnica de Catalunya

Av. Diagonal, 08028 Barcelona, Spain

A. Errachid

Université de Lyon, Laboratoire des Sciences Analytiques, CNRS, UMR 5180, Université Lyon 1, 43 boulevard du 11 novembre 1918, F-69622 Villeurbanne Cédex – France

Abstract

Calixarenes are promising compounds to be used as ionophores and for molecular recognition. Their ability to form Langmuir and Langmuir-Blodgett (LB) films is of great interest in order to obtain small sensor devices which incorporate an active nanometric film. The *p-tert*-butylcalix[7]arene ethyl ester compound has been synthesised and its ability to form Langmuir and LB films has been shown. This macrocycle forms monolayers but it tends to form multilayers at higher compressions, as corroborated by AFM. BAM images show a uniform layer till the multilayer process occurs and a good correspondence with the features of the surface pressure-area

isotherm. AFM images reveal that, in water subphase, films are quite homogeneous but the presence of small islands has also been observed. The presence of ions in the subphase, as sodium, potassium, rubidium, cesium, calcium, barium, cadmium and tin chloride salt solutions, leads to some changes in the surface pressure-area isotherms, but the more important changes are observed by AFM. More uniform films are observed for rubidium, cesium, cadmium and tin ions. A very different nanometric structure has been observed for tin ions. Some characteristics of the films, molecular area and height, are correlated with molecular modelling calculations.

Keywords

Calix[7]arene, Langmuir monolayer, Langmuir-Blodgett film, isotherm, AFM, ion influence, molecular modelling.

1. Introduction

Calixarenes are macrocyclic molecules built from phenolic units linked via methylene bridges. In the field of supramolecular chemistry, calixarenes are extremely popular building blocks for molecular recognition, forming host-guest complexes [1-3]. Calix[4]arenes are the most widely studied compounds in the calixarene family [4-16], although applications of calix[8]arenes [17,18], calix[6]arenes [18] or calix[3]arenes [19] have also been reported. The Langmuir technique has been used to study the response of calixarene derivative monolayers at metal ions present in the subphase [20-27], to amino acids [28] or for the molecular recognition of nucleosides [29]. Studies on Langmuir and Langmuir-Blodgett (LB) films of calix[4]arenes are more abundant than on calix[6]arenes [22,23,26] or calix[8]arenes [21,25,30,31]. Vollhardt et al. [27] studied the influence of diverse cations (Na^+, Cd^{2+}, Eu^{3+}, Th^{4+}) on amphiphilic P-functionalized calix[4]arene monolayers, concluding that the features of the isotherms are not influenced by the cations in the subphase, although Brewster Angle Microscopy (BAM) images show 2D condensed phase domains with a shape modified by the cation

valency. Davis et al. [21] studied the selective ion binding by LB films of calix[8]arenes and their derivatives with ethyl ester or methyl ketone groups in the lower rim. The authors found that these compounds form LB films readily and could determine the metal binding by X-ray photoelectron spectroscopy (XPS). Moreover, Yagi et al. [26] used the LB technique to study channel mimetic sensing membranes for alkali metal cations based on monolayers of calixarene esters. This process has been recently used to obtain a calixarenic modified electrode for the determination of lead and cadmium [7] or thallium and cadmium [32]. De Miguel et al. [31] have studied the organization of a calix[8]arene derivative at the air-water interface and Castillo et al. [30] the structure of Langmuir films of calix[8]arene/fullerene complexes. Recently, Roales et al. [33] investigated the optimization of mixed LB films of porphyrin in a calix[8]arene matrix for gas sensing application.

No studies have been reported on calix[7]arenes, except that of Markowitz et al. [34] who studied the permeation of water through films of mercurated calix[n]arenes, with n=4-7, and obtained Π-A isotherms of the films of these compounds. The authors concluded that the macrocycles form stable monolayers and that the limiting areas obtained from the Π-A isotherms are in agreement with the values predicted from space-filling models (CPK model) with the base parallel to the water surface. In order to get a deeper insight into the features of these calixarenes, we decided to synthesize and characterize the *p-tert*-butylcalix[7]arene ethyl ester. The formation of Langmuir films of this compound on water and different ion aqueous solution subphases was studied using surface pressure-area isotherms and BAM. These films were transferred to a solid substrate at several surface pressures, and the topographic and structural characteristics of the formed LB films were observed by using AFM. The influence of the ions on the characteristics of the films is discussed on the basis of the molecular structure of the calixarene and the size and charge of the ions. The potential ability of the *p-tert*-butylcalix[7]arene ethyl ester as ion sensor is also commented on the basis of the obtained results. For comparison purposes, films of the corresponding *p-tert*-butylcalix[4]arene ethyl ester have also been elaborated.

2. Experimental

Synthesis of p-tert-butylcalix[n]arene ethyl ester

All the organic and inorganic reagents used were pure commercial products. Acetone was distilled over $CaCl_2$ under nitrogen. Proton and ^{13}C NMR spectra were obtained on a Brucker AC 200 instrument. Mass spectrum was recorded on a VG ZAB2-SEQ at the Laboratory of Mass Spectrometry of the CNRS, Solaize, France.

The *p-tert*-butylcalix[7]arene ethyl ester (Figure 1, n=7), $C_{105}H_{140}O_{21}$ M=1738.17, was obtained from a procedure described previously for even calixarenes [4], but until now there is no report to the preparation of this compound. To the best of our knowledge, the synthesis of calixarenes with an odd number of phenolic units is less usual and more difficult. To a suspension of 2.18 g of K_2CO_3 (15.75 mmol) and 3.5 g of ethylbromoacetate (21 mmol) in acetone (15 mL), under nitrogen, were added 1.70 g of *p-tert*-butylcalix[7]arene (1.5 mmol) and 10 mL of acetone. The mixture was refluxed for three days and then it was filtered on silica plate. The filtrate was evaporated under vacuum and ethyl alcohol (50 mL) was added to the residue. After 24h at 0°C, the mix was filtered. The solid phase was purified by re-crystallisation (CH_2Cl_2/EtOH) to give 490 mg (0.28 mmol) of pure compound as white powder. Yield = 19 %. ^1H NMR (200 MHz, $CDCl_3$, 298 K): δ 7.06 (s, 14H, *H*-Ar); 4.16 (s, 14H, Ar-C*H*$_2$-Ar); 3.90-4.08 (m, 28H, Ar-O-C*H*$_2$-COO-C*H*$_2$-CH_3); 1.12 (s, 63H, Ar-C(CH_3)$_3$); 0.96 (t, 21H, Ar-O-CH_2-COO-CH_2-C*H*$_3$). ^{13}C NMR (50 MHz, CDCl3, 298 K): δ 168.99 (Ar-O-CH_2-*C*OO-CH_2-CH_3); 152.87 (Ar*C*-O); 146.55 (Ar*C*-C(CH_3)$_3$); 132.69 (Ar*C*-CH_2-Ar); 126.37 (Ar*C*-H); 70.13 (Ar-O-*C*H_2-COO-CH_2-CH_3); 60.79 (Ar-O-CH_2-COO-*C*H_2-CH_3); 34.20 (Ar-*C*(CH_3)$_3$); 31.42 (Ar-C(*C*H_3)$_3$); 30.56 (Ar-*C*H_2-Ar); 14.05 (Ar-O-CH_2-COO-*C*H_2-*C*H_3). Trimethylsilane (TMS) was used as the internal standard and the chemical shifts are given in ppm.

The *p-tert*-butylcalix[4]arene ethyl ester (Fig 1, n=4), $C_{60}H_{80}O_{12}$ M=993.24, was obtained as described previously [4].

Figure 1. Structure of *p-tert*-butylcalix[n]arene ethyl ester

Preparation of Langmuir and LB films

Langmuir films were obtained using a NIMA 1232D1D2 Langmuir-Blodgett trough (area=1200 cm^2) placed on an isolation platform and spreading a 0.575 mM (1 mg/mL) chloroform solution of the calix[7]arene, or a 1.007 mM (1 mg/mL) chloroform solution of the calix[4]arene, over the aqueous subphase which was MilliQ pure water (resistivity of 18 MΩ cm), or an aqueous solution containing one of the following salts: NaCl, KCl, RbCl, CsCl, $CaCl_2$, BaCl2, $CdCl_2$ or $SnCl_4$. Chemicals were of analytical grade. After solvent evaporation, the films were compressed. Barrier speeds of 50 or 25 cm^2/min, equivalent to 2.5 and 1.25 cm/min, respectively, were used to check the influence of the compression speed. Referred to one molecule, the compression speeds were between 7.2 and 16 $Å^2$/molecule/min. The surface pressure, Π, was measured with a Wilhelmy plate using paper that shows a null contact angle. BAM images were obtained using a NIMA-Nanofilm microBAM with a lateral resolution of around 8 μm.

LB films were deposited on freshly cleaved mica sheets of 1 cm x 1 cm, at a transfer speed of 5 mm/min (dipper velocity), and observed by AFM. The transfer was done from the corresponding films on water, using a NIMA 1232D1 dipper, at several surface pressures. LB films were obtained following a Z deposition, that is, the sheet of mica is first introduced into the subphase, and once the Langmuir film is formed, the mica sheet is pulled up. The obtained transfer ratios were close to 1, indicating a good transfer. AFM images were obtained with a Nanoscope IIIA (Digital Instruments, CA) using tapping mode, with silicon microfabricated cantilevers with a constant force of 40 N/m and 300 kHz frequency.

Molecular modelling studies

In order to understand the conformational features of the calix[4]arene and calix[7]arene, 10 ns molecular dynamics trajectories were conducted *in vacuo* using the parm99sb force field, embedded in the AMBER program [35]. The dielectric constant was set to 1 and no cutoff was used to compute the electrostatic interactions. The integration step was set to 1 fs. Snapshots of the trajectory were taken every ps and used

to compute atom-atom distances in order to characterize different average structural parameters of the molecules.

3. Results and discussion

Langmuir films were obtained from chloroform solutions of the calixarene compound. Figure 2a shows the Π-A isotherms in water subphase for the *p-tert*-butylcalix[7]arene ethyl ester, and also for comparison purposes that of the *p-tert*-butylcalix[4]arene ethyl ester. At first, the isotherm for the *p-tert*-butylcalix[7]arene ethyl ester shows a flat zone with Π=0 (zone I), a raising zone (zone II) and a quasi plateau (zone III) followed by subsequent raising part. The formation of a quasi plateau has also been reported by the authors in other type of macrocyclic compound [36, 37]. In the zone II one or two inflexions can be observed, the first at approximately Π=26 mN/m is more remarkable than the second one at approximately Π=31 mN/m, being the latter sometimes invisible. A similar shape is observed for the isotherm of the calix[4]arene with zones I, II and III, although without a clear inflexion in zone II. The plot of the Young modulus (K_S=-A(dΠ/dA)$_T$), versus the surface pressure (see Figure 2b) shows more clearly the inflexion points. For the calix[7]arene two inflexion points are clearly marked at the surface pressures indicated above. On the other hand, the values of K_S point to a liquid condensed (LC) state (100<K_S(LC)<250 m/mN) [38]. For the calix[4]arene inflexion points are not clearly marked, but a small inflexion appears at around 2 mN/m, which indicates a change from liquid expanded (LE, K_S(LE)<100 m/mN) to LC, and another small inflexion at around 9 mN/m, which corresponds to a change from LC to solid (S, K_S>250 m/mN) [38].

When short compressions are made, the reversing in zone II gives a reversible process, practically without hysteresis, and the reversing in the beginning in zone III is quite reversible, with small hysteresis (see Figure in Electronic Supplementary Information). After the reversing in the beginning of zone III and the process repeating, the form of the isotherms is practically the same, suggesting that the process is reversible. De Miguel et al. [31] have interpreted the differences found in recompression

on the basis of conformational changes of the substituted calixarenic molecules. In our case, the conformation of ethyl ester substituents can change in a similar way as described by these authors in the case of carboxylic acid substituents. The form of the isotherm is quite reproducible in different experiments and only small changes are observed at the end of zone II, where sometimes a less pronounced inflexion is observed. In regard to the influence of compression speed, our results indicate a small influence in the studied range.

The area value for the *p-tert*-butylcalix[7]arene ethyl ester at which zone II starts, ~2.5 nm^2, is in between those reported experimentally for the calix[6]arenes (2.06 nm^2 [20], 2.0 nm^2 [26], 1.80-2.00 nm^2 [22]) and those reported for some calix[8]arenes (2.70-4.40 nm^2 [25], 4.00-4.25 nm^2 [21]), but higher than those reported for another calix[8]arene (1.70-1.80 nm^2 [21]) or for a calix[7]arene (1.90-2.00 nm^2 [34]). On the other hand the experimental values sometimes agree with the calculated value by the CPK model supposing a parallel orientation of the rims in respect to water surface (flat-on), but sometimes the experimental values are lower inducing to consider a perpendicular orientation of the rims in respect to water (edge-on). Then a deeper discussion is needed for the value reported by us. In our case we have estimated the area using molecular dynamics simulations, as described in the experimental section. These simulations show that the calix[7]arene adopts elliptic conformations, with a major axe of 2.02 nm and a minor axe of 1.34 nm for the upper rim, the larger base corresponding to the hydrophobic side. For the purpose of calculation of an effective area, we consider that the molecule has the shape of a truncated cone, with the diameter of the upper rim of 1.68 nm, the mean value of the two reported axes (se Figure 3a). This value and the consideration of a compact arrangement (hexagonal packing) of the molecules in the flat-on orientation, provides an area of 2.44 nm^2. This value agrees with the experimental one.

The area value for the *p-tert*-butylcalix[4]arene ethyl ester at which zone II starts is ~ 1.35 nm^2, in close agreement with previous reported values (1.16 nm^2 Ishikawa [20], 1.1-1.6 nm^2 [26]), 1.02 nm^2 [27]). The area was estimated by us using molecular dynamics simulations. For this purpose, considering that the molecule has the shape of a truncated cone, we measured the diameter of upper rim, the larger base corresponding to the hydrophobic side. The average distance between two opposite *tert*-butyl groups is

1.33 nm (see Figure 3b). This distance, considered as the diameter of a circle, and the consideration of a compact arrangement of the molecules in the flat-on orientation, provides an area of 1.53 nm^2. This value agrees with the experimental one from the isotherm.

A small influence of the temperature is observed, with a small increase in the surface pressure of the plateau when the temperature decreases (see Figure 4). Usually it can be expected the opposite when a phase transition occurs, and suggests a sort of monolayer collapse due to a multilayer formation. This point will be discussed further below.

Figure 2a. Π-A isotherms of *p-tert*-butylcalix[n]arene ethyl esters, n=4 (left) and 7 (right), in water subphase at 25ºC and BAM images (2.5mm x 2.5mm).

Figure 2b. Young modulus versus the surface pressure for a film of *p-tert*-butylcalix[7]arene ethyl ester (♦) and *p-tert*-butylcalix[4]arene ethyl ester (■).

Figure 3. Molecular modelling calculations for the: a) *p-tert*-butylcalix[7]arene ethyl ester, b) *p-tert*-butylcalix[4]arene ethyl ester, c) conformational changes in the *p-tert*-butylcalix[7]arene ethyl ester measured as changes in the distances between two carbon (C) atoms of the *p-tert*-butyl groups, d1-4-C and d3-7-C, and between two oxygen (O) atoms of the carbonyl groups, d1-4-O and d3-7-O.

Figure 4. Π-A isotherms of *p-tert*-butylcalix[7]arene ethyl ester in water subphase at several temperatures: 18.5ºC (1), 22ºC (2) and 25ºC (3).

The second raising zone in the *p-tert*-butylcalix[7]arene ethyl ester isotherm, at lower areas (~ 1.25-1.3 nm^2) following the plateau (zone III), occurs at areas close to 1/2 of the first raising (~ 2.5 nm^2). This could indicate that the plateau corresponds to a bilayer formation. The bilayer formation is confirmed by AFM images of LB films

transferred in the plateau zone (see Figure 5a). Inspection of the Figure 5a shows that the second layer appears incomplete as domains or islands on top of the first layer (the formation of this first layer will be discussed and demonstrated later). The measured height of 1.3-1.4 nm for the second layer in respect to the first one corresponds to the monolayer height, which has also been calculated by us with the molecular model (see Figure 3a). For the *p-tert*-butylcalix[4]arene the observed areas are ~ 0.50-0.60 nm^2 and ~ 1.3-1.35 nm^2, respectively, indicating that probably a mixed bilayer-trilayer is formed in this case. Anyway, the formation of a multilayer seems clear in both cases. Yagi et al. [26], working with *p-tert*-butylcalix[4]arene ethyl ester have also observed the beginning of zone III at a surface pressure of ~ 25 mN/m, in agreement with our observation (see Figure 2), although they do not report a wide plateau. Other studies indicate that the *p-tert*-octylcalix[4]arene ethyl ester shows a plateau at around 22 mN/m and the *p-tert*-butylcalix[6]arene ethyl ester also shows a plateau at around 35 mN/m, and in both cases it seems that the plateau ends at an area half of that of the beginning, indicating probably a bilayer formation. For our *p-tert*-butylcalix[7]arene ethyl ester the plateau occurs at nearly 37-38 mN/m. Davis et al [21] also observed an inflexion in the isotherm of a calix[8]arene ethyl ester at a surface pressure of around 30 mN/m, but the isotherm is truncated at this point and no plateau formation is shown. Also in this paper the isotherm for the non-substituted calix[8]arene is shown, which present an inflexion at around 15 mN/m, indicating that the surface pressure value at what this process occurs will depend on the ring size and the substituents.

The influence of temperature on the surface pressure of the inflexion observed in zone II, at around 26 mN/m, is also small, with a small increase in the surface pressure of the inflexion when temperature decreases (see Figure 4). This observation seems to indicate a sort of partial monolayer collapse due to a multilayer formation and not due to a phase transition. This point is also confirmed by AFM images of LB films transferred at Π>26 mN/m (Figure 5b), where small islands can be seen. These islands are smaller than in Figure 5a and lesser in number, but with a similar height around 1.3 nm.

Figure 5. AFM images (area 0.7μm x 0.7μm (a) and 1.0μm x 1.0μm (b)) of LB films of *p-tert*-butylcalix[7]arene ethyl ester, in water subphase, transferred at: (a) the plateau (zone III), (b) 32 mN/m, with the corresponding profile sections.

This partial monolayer collapse at around 26 mN/m may be induced by conformational changes in the *p-tert*-butylcalix[7]arene ethyl ester, as molecular dynamics calculations show that they occur (Figure 3c). These calculations show that the distances between two selected atoms change with time. These conformational changes do not occur in the *p-tert*-butylcalix[4]arene ethyl ester and then no inflexions as those observed in the *p-tert*-butylcalix[7]arene ethyl ester are observed. For the calix[6]arene, Ishikawa et al. [20] also observed a weak inflexion in the isotherm at a surface pressure around 25 mN/m, more similar to that observed by us for the calix[7]arene, and a great inflexion for the calix[8]arene at a surface pressure 18 mN/m. In this sense, the calix[7]arene behaves more similar to the calix[6]arene than to the calix[8]arene. In the authors' opinion, the conformational changes favour the slipt-out of some molecules from the monolayer due to the increasing surface pressure, leading to an inflexion in the isotherm. As the conformational changes are temperature dependent, lower surface pressures are needed at higher temperatures to produce the slip-out, which is observed experimentally.

The films show good stability, and the area decrease is only of 2.2% after 40 min at Π=30 mN/m and in water subphase. This value is even less at lower surface pressures. Isotherm cycles show a certain irreversibility with some hysteresis in the isotherms, more important if we arrive at the end of the plateau at medium compressions (at high compressions the process is very irreversible). Nevertheless the fact that reproducible isotherms are obtained in successive compressions, after a relaxing time of 10 min, indicates that it is only a kinetic question: with enough time molecules recover the initial state, the aggregation and multilayer formation are reversible in zone III. The hysteresis phenomenon is usually seen when multilayering or collapsing of the films occurs.

BAM images (see Figure 2) show a uniform film in zone II of the isotherm but with some stripes or irregularities at around 26 mN/m for the *p-tert*butylcalix[7]arene

ethyl ester; this value corresponds to the inflexion observed in the Π-A isotherm. The second inflexion observed around 31 mN/m is manifested in the BAM with brighter stripes. Probably, and according to AFM images and the fact that a small increase in the surface pressure of the inflexion occurs when temperature decreases, these inflexions shows the beginning of a partial formation of a multilayer with the slip out of the monolayer. This process follows in zone III, the plateau. The nanometric size domain observed by AFM (Figure 5) is out of the resolution of the used BAM. This multilayer formation has also been observed in BAM images for a calix[8]arene [30] but yet at low surface pressure values; for this system the authors stated that the film is in a solid phase and that a transition from gas to solid phase occurs. In our case the appearance and behaviour of the film on zone II, with a value of the Young modulus around 200 mN/m for the *p-tert*-butylcalix[7]arene ethyl ester, points to a liquid condensed (LC) phase, and multilayering occurs at higher surface pressure values. De Miguel et al. [31] also obtained BAM images for the carboxylic-acid-substituted calix[8]arene, which differently show the presence of a solid phase that on decompression breaks and forms small branchlike domains; in our system no breaks in small domains were observed, which is in agreement with the presence of a more fluid phase. Thus, the different molecular structure of our compound, being the calixarene ring size, the substituents or both, have an important role on the characteristics of the film. Ester groups will interact weaker with water and with other ester groups than do carboxylic or alcohol groups (forming hydrogen bounds), leading to a more fluid phase. These weaker interactions can also explain the more facility in the formation of a multilayer.

Figure 6 shows AFM images for the *p-tert*-butylcalix[7]arene ethyl ester with the characteristics of LB films transferred from water subphase and surface pressures of 20 and 32 mN/m, revealing the nanometric structure of the films and the influence of the transfer surface pressure. Films are quite homogeneous and smooth, but at Π=32 mN/m the image shows the presence of very small islands increasing in height and number in comparison with those at Π=20 mN/m. The monolayer height at Π=20 mN/m was determined after scratching the film by the profile of the topographic AFM image, obtaining a value of 1.3-1.4 nm, which corresponds with the value calculated from the molecular model (Figure 3a).

Aged LB samples for the *p-tert*-butylcalix[7]arene ethyl ester show small changes, indicating the stability of the LB films, except those transferred at the plateau zone that present notable changes.

Figure 6. AFM images (area 2.0μm x 2.0μm) of LB films of *p-tert*-butylcalix[7]arene ethyl ester transferred at Π=20 mN/m (A) and 32 mN/m (B).

Subphase influence

The influence of different ions in solution has been investigated. Surface pressure-area isotherms were recorded and AFM of LB films were obtained for different ionic subphases: NaCl, KCl, RbCl, CsCl, $CaCl_2$, $BaCl_2$, $CdCl_2$ and $SnCl_4$. The ions in the alkaline or alkaline-earth series show different values of the ionic radius, while Na, Ca, Cd and Sn ions show more similar values but with different charges (Table 1).

Table 1. Ionic radii (Å) of the investigated cations [C-S. Zuo, O. Wiest, Y-D. Wu, J. Phys. Chem. A 113 (2009) 12028]

Cation	Na^+	K^+	Rb^+	Cs^+	Ca^{2+}	Ba^{2+}	Cd^{2+}	Sn^{4+}
From Pauling (a)	0.95	1.33	1.48	1.69	0.99	1.35	0.97	0.71
From Marcus (b)	1.02	1.38	1.49	1.70	1.00	1.36	0.95	

(a) L. Pauling, "The Nature of the Chemical Bond", 3rd ed. 1960.

(b) Y. Marcus, J. Chem. Soc. Faraday Trans. 87 (1991) 2995.

For the series of alkaline cations there are little differences in the isotherms, at 22ºC, showing all of them the same shape (Figure 7), which is also similar to that of water, and only a slight displacement in the area axis is observed. AFM images of LB films transferred at Π=20 mN/m show more uniform films for Rb and Cs ions (Figure 8). Analyzing the images of Figure 8 it is obtained that the mean roughness and standard deviation are, respectively, 0.187 nm and 0.420 nm for Na, 0.169 nm and 0.297 nm for K, 0.068 nm and 0.094 nm for Rb and 0.132 nm and 0.206 nm for Cs.

Figure 7. Π-A isotherms, at 22ºC, of *p-tert*-butylcalix[7]arene ethyl ester at different 0.01M subphases of alkaline ion salts: NaCl (grey 50%), KCl (black thin), RbCl (black thick), CsCl (grey 25%).

Figure 8. AFM images (area 2.0μm x 2.0μm) of LB films of *p-tert*-butylcalix[7]arene ethyl ester transferred at Π=20 mN/m from different alkaline ion subphases.

For the divalent cations the shape of the isotherms at 22ºC is also similar except the presence of some differences in the rising area of zone II, the slope or the plateau pressure (Figure 9). The isotherm for the calcium subphase attains the plateau at a slightly higher surface pressure. AFM images of LB films at 20 mN/m show more uniform films for the Cd ions (Figure 10). The mean roughness and standard deviation analyzing image of Figure 10, are, respectively, 0.107 nm and 0.143 nm for Cd. The LB films for Ca and Ba present some islands but comparing the AFM images for the monovalent ions Na and K with those of the divalent ions Ca and Ba, it seems that the films for the latter are slightly more uniform since the number of islands is less, but a statistical analysis indicates no much differences between them: the mean roughness and standard deviation analyzing images of Figures 8 and 10 are, respectively, 0.187 nm and 0.420 nm for Na, 0.169 nm and 0.297 nm for K, 0.255 nm and 0.389 nm for Ca and 0.143 nm and 0.277 nm for Ba; the Ba ions films seem to be slightly more uniform.

AFM images of LB films at 20 mN/m show uniform films for the Sn ions but with a granular structure in the nanometric scale (see Figure 10), being in this sense different to those of the other ions, and a statistically roughness analysis gives values of mean roughness and standard deviation of, respectively, 0.552 nm and 0.700 nm.

Figure 9. Π-A isotherms, at 22ºC, of *p-tert*-butylcalix[7]arene ethyl ester at different 0.01M subphases of divalent ion salts: $CaCl_2$ (grey 25%), $BaCl_2$ (grey 50%), $CdCl_2$ (black).

Figure 10. AFM images (area 2.0μm x 2.0μm) of LB films of *p-tert*-butylcalix[7]arene ethyl ester transferred at Π=20 mN/m from different divalent (Ca, Ba, Cd) and tetravalent (Sn) ion subphases.

For the series of Na, Ca, Cd and Sn cations, at 22ºC, there are also some differences in the isotherms (Figure 11). The isotherms of Na and Ca cations are more similar, with only one marked inflexion in zone II, meanwhile the isotherm of Cd cation shows two marked inflexions in zone II. The isotherm of Sn cation present a slight higher slope in zone II with nearly no inflexion, reaching a slight higher value of the surface pressure at the plateau, as calcium cations subphase does.

The isotherms in ion subphases show also the plateau reported previously in water subphase. The area at the second raising zone at lower areas, following the plateau (zone III), also occurs at areas close to 1/2 of the first raising and, as discussed above, this indicates that the plateau corresponds to the formation of a bilayer. This phenomenon is observed in all subphases with a small influence of the subphase in the surface pressure at which it occurs. One would expect a larger influence of ions since the calixarene does interact with them. However, if ions place in the cavity of the calixarene ring, the complex ion-calixarene will behave similar to the calixarene molecule in the process of film formation. This behaviour has been observed for other calixarene-metal complexes and even for a calixarene-C_{60} complex [30]. Nevertheless, the isotherm obtained in ions subphase is steeper than in water subphase, and thus with slightly lower compressibility coefficients, indicating that the ions placed in the calixarene cavity impart more rigidity to the molecule.

Figure 11. Π-A isotherms, at 22ºC, of *p-tert*-butylcalix[7]arene ethyl ester at different 0.01M subphases of ion salts: $CaCl_2$ (grey 25%), NaCl (grey 50%), $CdCl_2$ (black thin), $SnCl_4$ (black thick).

In some aspects, our results agree with those of the work of Vollhardt et al [27] where it was also stated that isotherms of monolayers of a P-functionalized calix[4]arene showed the same characteristics in subphases containing different cations as Na^{+}, Cd^{2+}, Eu^{3+}, Th^{4+} but the BAM images showed 2D condensed phase domains with a shape modified by the cation valency.

AFM images at Π=32 mN/m show for all the ionic subphases the presence of a bigger number of islands, as occurred with the water subphase, except for the tin ion subphase. This fact can be related to the practically absence of inflexion in zone II of the isotherm for tin subphase. Also the appearance of the multilayer, in the plateau, is different for the tin subphase, showing the granular aspect, meanwhile the rest of ions present the multilayer formation as for water subphase (see Figure 5a).

There is a small influence of temperature on the isotherms with salt subphase. The isotherms at the lower temperature of 22ºC generally show a more pronounced first inflexion in zone II, at around 26 mN/m, with practically no second inflexion, meanwhile the isotherms at the higher temperature of 25ºC (Figure 12) generally show weak inflexions. According to our explanation, at lower temperature the film is more rigid and the conformational changes can produce a higher effect in the film compactness and a more marked effect in the slipt-out of the molecules and consequently a more marked inflexion.

Figure 12. Π-A isotherms, at 25ºC, of *p-tert*-butylcalix[7]arene ethyl ester at different subphases: water (1), and 0.01M ion salts: $CdCl_2$ (2), $CaCl_2$ (3) and NaCl (4).

4. Conclusions

A compound in the family of calixarenes, a *p-tert*-butylcalix[7]arene ethyl ester, has been synthesised and its capability to form Langmuir and LB films has been assessed.

After a certain surface pressure a multilayer process occurs, which is seen in the isotherm by the presence of a plateau. Inflexions in the isotherm at surface pressures lower than that of the plateau can be induced by conformational changes in the *p-tert*-butylcalix[7]arene ethyl ester molecule, as molecular dynamics calculations show.

The influence of several ions present in the subphase has been tested, in order to check the interactions with the compound. These ions show some changes in the isotherms, but as the changes are not dramatic they also indicate that the ions placed in the calixarene cavity due to its small size. Some changes are also observed in the film formation by AFM. The presence of more uniform films for some ions indicates a stronger binding of the calixarene molecules, and consequently a more difficult slipt-out of these molecules, at less at the surface pressure of 20 mN/m. More research will be done in future for analyzing the influence of other factors and the sensing character.

Acknowledgements

We would like to acknowledge the Spanish Ministry of Science and Technology for financial support through the project CTQ2007-68101-C02-02.

References

[1] Calixarenes in the nano world, Edited by J. Vicens, J. Harrowfield and L. Baklouti, Springer, Dordrecht, 2007.

[2] C. D. Gutsche, Calixarenes Revisited, Publisher: Royal Soc. Chem., Letchworth, UK, 1998.

[3] Z. Asfari, V. Böhmer, J.M. Harrowfield, J. Vicens, in Calixarenes 2001, Kluwer Academic Publishers, Dordrecht, 2001.

[4] F. Arnaud-Neu, E. M. Collins, M. Deasy, G. Ferguson, S. J. Harris, B. Kaitner, A. J. Lough, M. A. McKervey, E. Marques, Synthesis, x-ray crystal structures, and cation-binding properties of alkyl calixaryl esters and ketones, a new family of macrocyclic molecular receptors, J. Am. Chem. Soc. 111 (1989) 8681.

[5] M. Benounis, N. Jaffrezic-Renault, H. Halouani, R. Lamartine, I. Dumazet-Bonnamour, Detection of heavy metals by an optical fiber sensor with a sensitive cladding including a new chromogenic calix[4]arene molecule, Mater. Sci. Engin. C 26 (2006) 364.

[6] M. Ben Ali, R. Ben Chabanne, F. Vocanson, C. Dridi, N. Jaffrezic, R. Lamartine, Comparison study of evaporated thiacalix[4]arene thin films on gold substrates as copper ion sensing, Thin Solid Films 495 (2006) 368.

[7] H. Zheng, Z. Yan, H. Dong, B. Ye, Simultaneous determination of lead and cadmium at a glassy carbon electrode modified with Langmuir-Blodgett film of *p-tert*-butylthiacalix[4]arene, Sens. Actuators B 120 (2007) 603.

[8] I.A. Marques de Oliveira, D. Risco, F. Vocanson, E. Crespo, F. Teixidor, N. Zine, J. Bausells, J. Samitier, A. Errachid, Sodium ion sensitive microelectrode based on a *p-tert*-butylcalix[4]arene ethyl ester, Sens. & Actuators B 130 (2008) 295.

[9] N. Zine, J. Bausells, F. Vocanson, R. Lamartine, Z. Asfari, F. Teixidor, E. Crespo, I.A. Marques de Oliveira, J. Samitier, A. Errachid, Potassium-ion selective solid contact microelectrode based on a novel 1,3-(di-4-oxabutanol)-calix[4]arene-crown-5 neutral carrier, Electrochim. Acta 51 (2006) 5075.

[10] A. Rouis, R. Mlika, J. Davenas, H.B. Ouada, I. Bonnamour, N. Jaffrezic, Impedance spectroscopy investigations of ITO modified by new azo-calix[4]arene immobilised into electroconducting polymer (MSHPPV), J. Electroanal. Chem. 601 (2007) 29.

[11] A. Rouis, R. Mlika, C. Dridi, J. Davenas, H.B. Ouada, H. Halouani, I. Bonnamour, N. Jaffrezic, Optical spectroscopy studies of the complexation of chromogenic azo-calix[4]arene with Eu^{3+}, Ag^{+} and Cu^{2+} ions, Mater. Sci. Engin. C 26 (2006) 247.

[12] W. Ngeontae, W. Janrungroatsakul, N. Morakot, W. Aeungmaitrepirom, T. Tuntulani, Novel potentiometric approach in glucose biosensing using silver nanoparticles as redox matter, Sens. & Actuators B 137 (2009) 320.

[13] T. Ceyhan, A. Altindal, A.R. Ozkaya, M.K. Erbil, O. Bekaroglu, Synthesis, characterization and electrochemical, electrical and gas sensing properties of a novel *p-tert*-butylcalix[4]arene bridged bis double-decker lutetium(III) phthalocyanine, Polyhedron 26 (2006) 73.

[14] V.D. Vaze, A.K. Srivastava, Determination of pyridoxine hydrochloride in pharmaceutical preparations by calixarene based potentiometric sensor, J. Pharmaceutical Biomed. Analysis 47 (2008) 177.

[15] V.D. Vaze, A.K. Srivastava, Electrochemical behaviour of folic acid at calixarene based chemically modified electrodes and its determination by adsorptive stripping voltammetry, Electrochim. Acta 53 (2007) 1713.

[16] B-L. Su, X-C. Ma, F. Xu, L-H. Chen, Z-Y. Fu, N. Moniotte, S.B. Maamar, R. Lamartine, F. Vocanson, SBA-15 mesoporous silica coated with macrocyclic calix[4]arene derivatives: solid extraction phases for heavy metal ions, J. Colloid Interf. Sci. 360 (2011) 86.

[17] V. Huc, K. Pelzer, A new specifically designed calix[8]arene for the synthesis of functionalized, nanometric and subnanometric Pd, Pt and Ru nanoparticles, J. Colloid Interf. Sci. 318 (2008) 1.

[18] T. Katsu, N. Okaki, K. Watanabe, K. Takaishi, H. Yokosu, Comparative study of the response of membrane electrodes based on calix[6]arene and calix[8]arene derivatives to organic ammonium ions, Anal. Sci. 19 (2003) 771.

[19] G. Herzog, B. McMahon, M. Lefoix, N.D. Mullins, C.J. Collins, H.A. Moynihan, D.W.M. Arrigan, Electrochemistry of dopamine at the polarised liquid/liquid interface facilitated by an homo-oxo-calix[3]arene ionophore, J. Electroanal. Chem. 622 (2008) 109.

[20] Y. Ishikawa, T. Kunitake, T. Matsuda, T. Otsuka, S. Shinkai, Formation of calixarene monolayer which selectively respond to metal ions, J. Chem. Soc. Chem. Commun. (1989) 736.

[21] F. Davis, L.O'Toole, R. Short, C.J.M. Stirling, Selective ion binding by Langmuir-Blodgett films of calix[8]arenes, Langmuir 12 (1996) 1892.

[22] L. Dei, A. Casnati, P.L. Nostro, P. Baglioni, Selective complexation by *p-tert*-butylcalix[6]arene in monolayers at the water-air interface, Langmuir 11 (1995) 1268.

[23] L. Dei, A. Casnati, P.L. Nostro, A. Pochini, R. Ungaro, P. Baglioni, Complexation properties of *p-tert*-butylcalix[6]arene hexamide in monolayers at the water-air interface, Langmuir 12 (1996) 1589.

[24] Z. Ye, S. Pang, W. He, X. Shi, Z. Guo, L. Zhu, Copper(II) ion induced monolayer formation of *p-tert*-butylthiacalix[4]arene at the air-water interface, Spectrochim. Acta A 57 (2001) 1443.

[25] B. Lonetti, E. Fratini, A. Casnati, P. Baglioni, Langmuir monolayers of calix[8]arene derivatives: complexation of alkaline earth ions at the air/water interface, Colloids Surf. A 248 (2004) 135.

[26] K. Yagi, S.B. Khoo, M. Sugawara, T. Sakaki, S. Shinkai, K. Odashima, Y. Umezawa, Channel mimetic sensing membranes for alkali metal cations based on oriented monolayers of calixarene esters, J. Electroanal. Chem. 401 (1996) 65.

[27] D. Vollhardt, J. Gloede, G. Weidemann, R. Rudert, Characteristic features of amphiphilic P-Functionalized calixarene monolayers at the air/water interface, Langmuir 19 (2003) 4228

[28] M.W. Sugden, T.H. Richardson, F. Davis, S.P.J. Higson, C.F.J. Faul, Langmuir and Langmuir-Blodgett properties of two calix[4]resorcinarenes: interactions with various analytes, Colloids Surf. A 321 (2008) 43.

[29] X. Guo, G-Y. Lu, Y. Li, Interaction between calix[4]arene derivative bearing adenino units and complementary nucleosides at the air-water interface, Thin Solid Films 460 (2004) 264.

[30] R. Castillo, S. Ramos, R. Cruz, M. Martinez, F. Lara, J. Ruiz-Garcia, Langmuir films of calix[8]arene/fullerene complexes, J. Phys. Chem. 100 (1996) 709.

[31] G. de Miguel, J.M. Pedrosa, M.T. Martín-Romero, E. Muñoz, T.H. Richardson, L. Camacho, Conformational changes of a calix[8]arene derivative at the air-water interface, J. Phys. Chem. B 109 (2005) 3998.

[32] H. Dong, H. Zheng, L. Lin, B. Ye, Determination of thallium and cadmium on a chemically modified electrode with Langmuir-Blodgett film of *p*-allylcalix[4]arene, Sens. Actuators B 115 (2006) 303.

[33] J. Roales, J.M. Pedrosa, P. Castillero, M. Cano, T.H. Richardson, Optimization of mixed Langmuir-Blodgett films of a water insoluble porphyrin in a calixarene matrix for optical gas sensing, Thin Solid Films 519 (2011) 2025.

[34] M.A. Markowitz, V. Janout, D.G. Castner, S.L. Regen, Perforated monolayers: design and synthesis of porous and cohesive monolayers from mercurated calix[n]arenes, J. Am. Chem. Soc. 111 (1989) 8192.

[35] D.A. Case, T.A. Darden, T.E. Cheatham, III, C.L. Simmerling, J. Wang, R.E. Duke, R. Luo, R.C. Walker, W. Zhang, K.M. Merz, B.P. Roberts, B. Wang, S. Hayik, A. Roitberg, G. Seabra, I. Kolossváry, K.F. Wong, F. Paesani, J. Vanicek, J. Liu, X. Wu, S.R. Brozell, T. Steinbrecher, H. Gohlke, Q. Cai, X. Ye, J. Wang, M.-J. Hsieh, G. Cui, D.R. Roe, D.H. Mathews, M.G. Seetin, C. Sagui, V. Babin, T. Luchko, S. Gusarov,

A. Kovalenko, P.A. Kollman (2010), *AMBER 11*, University of California, San Francisco.

[36] J. Torrent-Burgués , M. Pla, L. Escriche, J. Casabó, A. Errachid, F. Sanz, Characterization of Langmuir and Langmuir-Blodgett films of a thiomacrocyclic ionophore by surface pressure and AFM, J. Colloid Interf. Sci. 301 (2006) 585.

[37] G. Oncins, J. Torrent-Burgués, F. Sanz, Lateral force microscopy study of Langmuir-Blodgett films of a macrocyclic compound, Tribology Letters 21 (2006) 175.

[38] a) J.T. Davies, E.K. Rideal, Interfacial phenomena, Academic Press, NY 1993. b) J. Torrent-Burgués, Phase separation in mixed monolayers of arachidic acid and a phthalocyanine of zinc, Colloids Surf. A 396 (2012) 137.

Captions for Figures

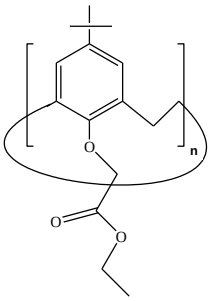

Figure 1. Structure of *p-tert*-butylcalix[n]arene ethyl ester

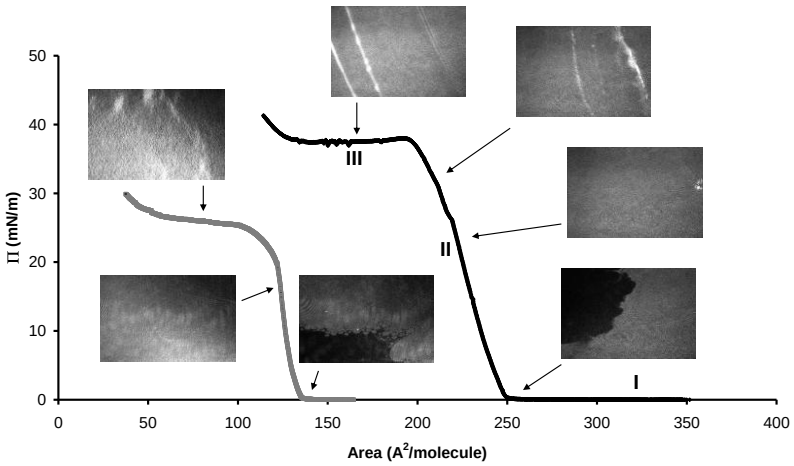

Figure 2a. Π-A isotherms of *p-tert*-butylcalix[n]arene ethyl esters, n=4 (left) and 7 (right), in water subphase at 25ºC and BAM images (2.5x2.5 mm).

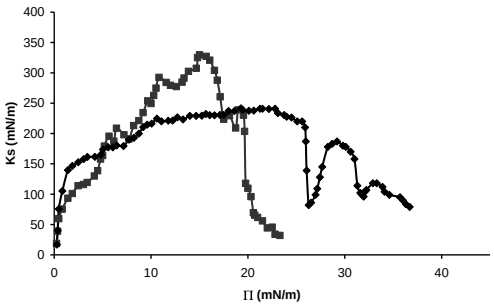

Figure 2b. Young modulus versus the surface pressure for a film of *p-tert*-butylcalix[7]arene ethyl ester (♦) and *p-tert*-butylcalix[4]arene ethyl ester (■).

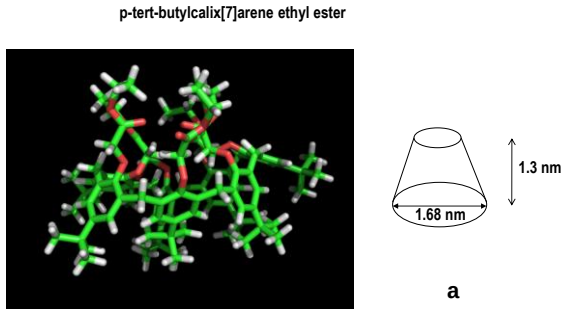

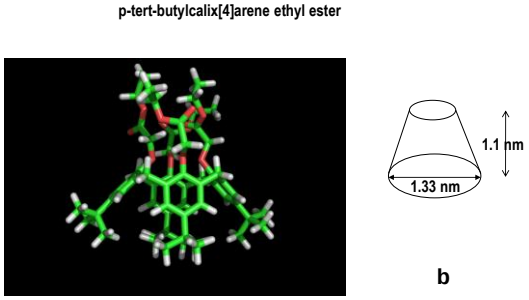

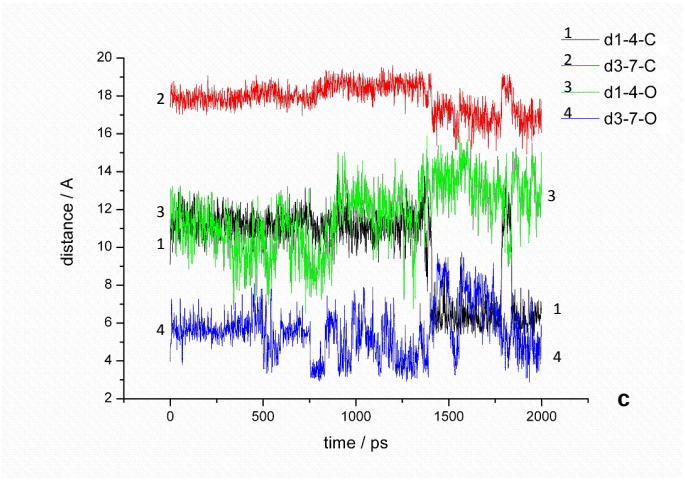

Figure 3. Molecular modelling calculations for the: a) *p-tert*-butylcalix[7]arene ethyl ester, b) *p-tert*-butylcalix[4]arene ethyl ester, c) conformational changes in the *p-tert*-butylcalix[7]arene ethyl ester measured as changes in the distances between two carbon (C) atoms of the *p-tert*-butyl groups, d1-4-C and d3-7-C, and between two oxygen (O) atoms of the carbonyl groups, d1-4-O and d3-7-O.

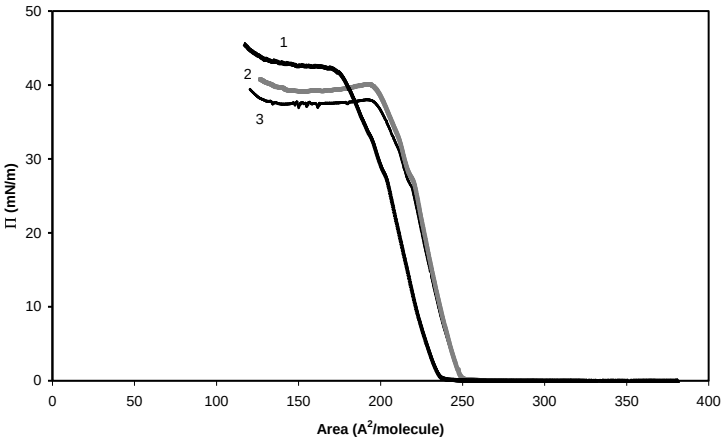

Figure 4. Π-A isotherms of *p-tert*-butylcalix[7]arene ethyl ester in water subphase at several temperatures: 18.5ºC (1), 22ºC (2) and 25ºC (3).

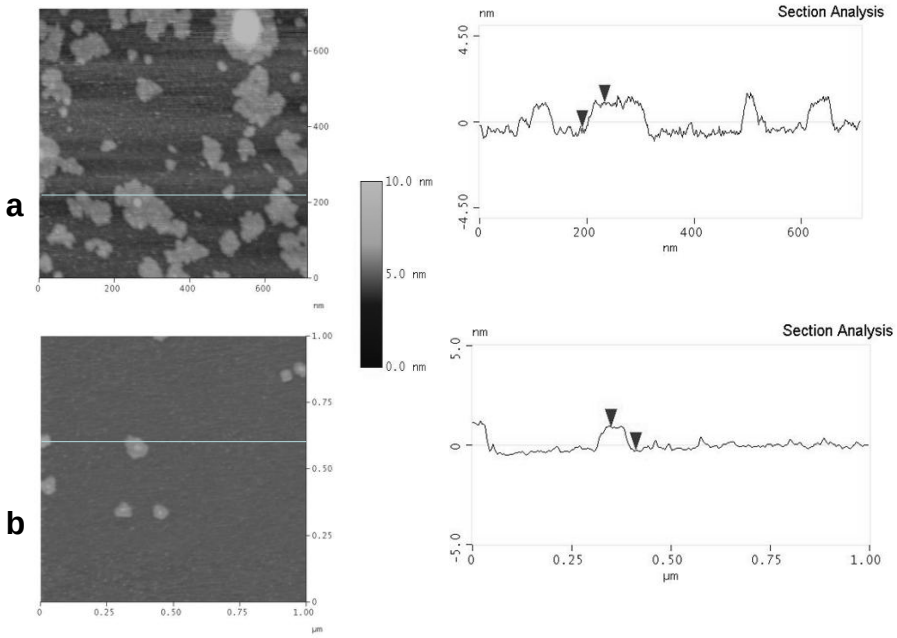

Figure 5. AFM images (area 0.7µm x 0.7µm (a) and 1.0µm x 1.0µm (b)) of LB films of *p-tert*-butylcalix[7]arene ethyl ester, in water subphase, transferred at: (a) the plateau (zone III), (b) 32 mN/m, with the corresponding profile sections.

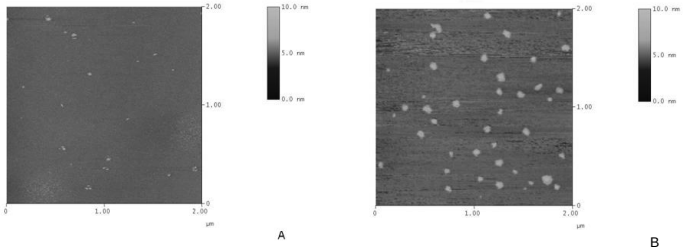

Figure 6. AFM images (area 2.0μm x 2.0μm) of LB films of *p-tert*-butylcalix[7]arene ethyl ester transferred at Π=20 mN/m (A) and 32 mN/m (B).

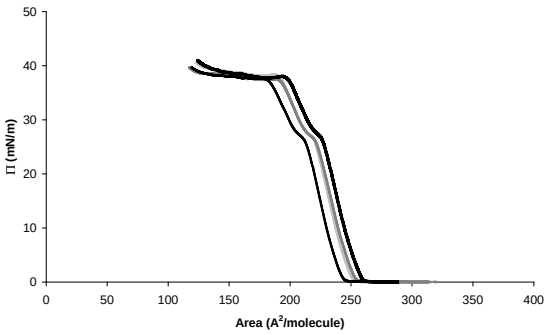

Figure 7. Π-A isotherms, at 22ºC, of *p-tert*-butylcalix[7]arene ethyl ester at different 0.01M subphases of alkaline ion salts: NaCl (grey 50%), KCl (black thin), RbCl (black thick), CsCl (grey 25%).

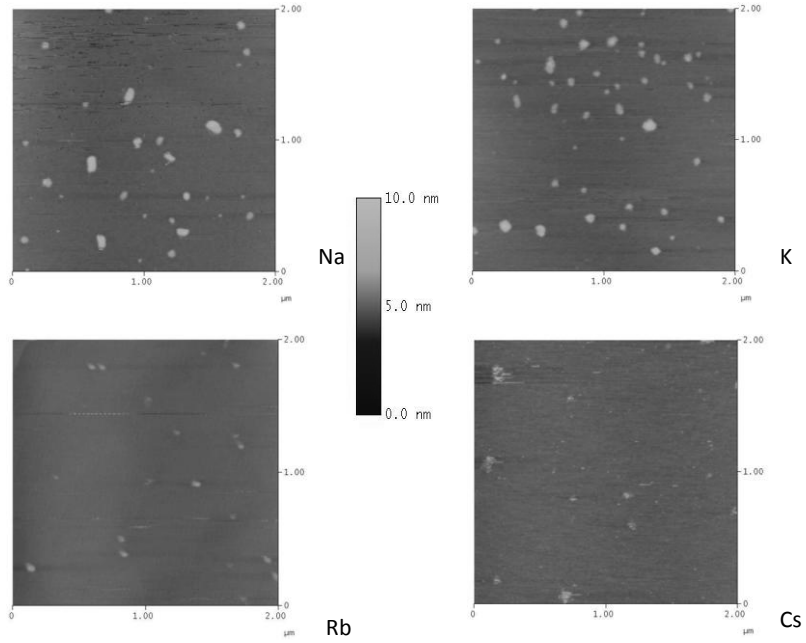

Figure 8. AFM images (area 2.0μm x 2.0μm) of LB films of *p-tert*-butylcalix[7]arene ethyl ester transferred at Π=20 mN/m from different alkaline ion subphases.

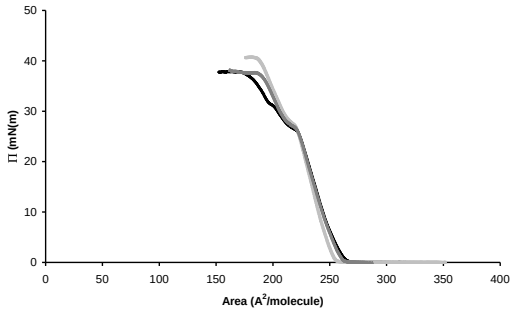

Figure 9. Π-A isotherms, at 22ºC, of *p-tert*-butylcalix[7]arene ethyl ester at different 0.01M subphases of divalent ion salts: $CaCl_2$ (grey 25%), $BaCl_2$ (grey 50%), $CdCl_2$ (black).

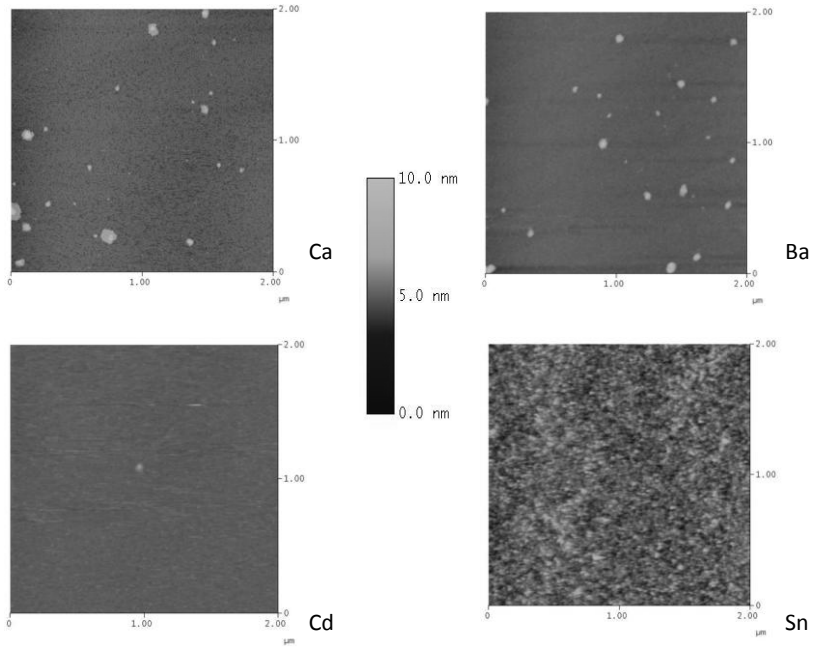

Figure 10. AFM images (area 2.0μm x 2.0μm) of LB films of *p-tert*-butylcalix[7]arene ethyl ester transferred at Π=20 mN/m from different divalent (Ca, Ba, Cd) and tetravalent (Sn) ion subphases.

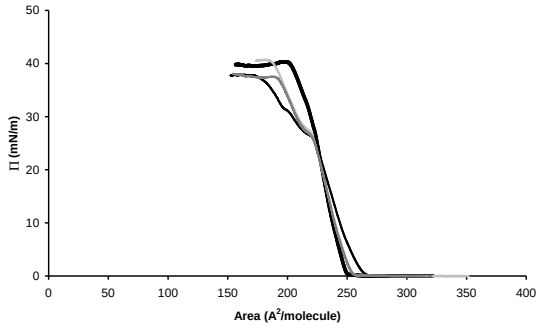

Figure 11. Π-A isotherms, at 22ºC, of *p-tert*-butylcalix[7]arene ethyl ester at different 0.01M subphases of ion salts: $CaCl_2$ (grey 25%), NaCl (grey 50%), $CdCl_2$ (black thin), $SnCl_4$ (black thick).

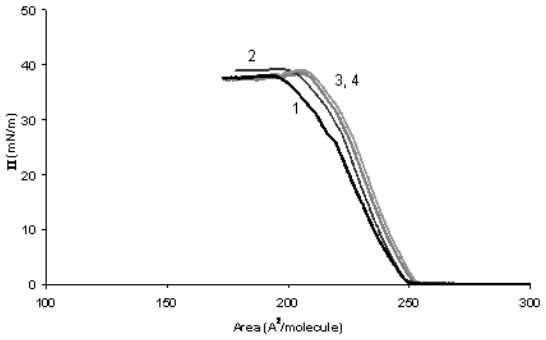

Figure 12. Π-A isotherms, at 25ºC, of *p-tert*-butylcalix[7]arene ethyl ester at different subphases: water (1), and 0.01M ion salts: $CdCl_2$ (2), $CaCl_2$ (3) and NaCl (4).